First-order breaking transition of tilted nematic anchoring

I. Dozov* and Ph. Martinot-Lagarde
Laboratoire de Physique des Solides, Université Paris–Sud, Bâtiment 510, 91405 Orsay Cedex, France
(Received 1 June 1998)

We propose a mechanism for breaking tilted nematic anchorings using an electric field normal to the plates. This breaking is a discontinuous first-order transition, unlike the known second-order breaking of planar anchorings. The elastic coupling of the tilted orientations on both plates is used to initialize the first-order transition. We observe the breaking experimentally by fast (in the μs range) bulk texture changes, resulting in an additional π twist in the final state. [S1063-651X(98)05312-4]

PACS number(s): 61.30.−v 42.79.Kr

The anchoring of liquid crystals on solid substrates is an important subject from both academic and applied points of view. Most of the actual liquid crystal devices require very strong anchoring energy and during their operation the orientation of the nematic director $\mathbf{n}_s$ close to the substrate remains unchanged. However, several devices have been proposed using weak anchorings, enabling the reorientation of $\mathbf{n}_s$ under strong external fields. In particular, ferroelectric C^* [1] and nematic [2–5] bistable displays have been demonstrated, based on *breaking* of the anchoring: under high enough field the surface director $\mathbf{n}_s$ passes through an anchoring energy *maximum* and after the pulse can go back to a new orientation. For monostable anchorings [5] the only possible change of orientation is a rotation of the surface director by π. Although locally the states $\mathbf{n}_s$ and $-\mathbf{n}_s$ are equivalent, this π rotation creates a new bulk texture, different from the initial one by half-turn distortion.

For planar orientation (with strictly zero tilt) the anchoring breaking was predicted and observed 15 years ago [6,7]. By symmetry arguments, this is a second-order transition and it cannot exist for tilted anchorings. Here we show that anchoring breaking is possible also in the case of tilted orientations, giving a first-order anchoring transition. We present experimental evidence for this first-order breaking in the case of tilted anchoring of 5CB on SiO.

Let us first consider monostable anchoring of a nematic on a flat substrate at $z=0$ in a semi-infinite sample. In the following we suppose a dielectrically positive material ($\epsilon_a = \epsilon_\parallel - \epsilon_\perp > 0$) and electric field $\mathbf{E}$, applied along the surface normal $\mathbf{N}\|\mathbf{z}$ (the only direction along which it is easy to apply a strong field in a thin cell). Without external torque, $\mathbf{n}_s$ is along the substrate easy axis $\mathbf{e}$ (Fig. 1), the minimum of the anchoring energy, and we suppose that it remains always in the plane xz, because only zenithal torques are applied to the director. The director is then $\mathbf{n}(z)=(\sin\theta,0,\cos\theta)$, where $\theta=\theta(z)$. In Fig. 1 we also show the direction $\mathbf{d}$ (''difficult'' axis), along which the anchoring energy has a maximum. For simplicity, we assume here a Rapini-Papoular [8] form of the anchoring energy:

$$W(\theta)=\frac{1}{2}A\sin^2(\theta_s-\theta_e), \tag{1}$$

where A is the zenithal anchoring strength and $\theta_s=\theta(z=0)$. This approximation will greatly simplify our approach, for example, giving automatically $\mathbf{d}\perp\mathbf{e}$, but it should be used with caution: we will show in the discussion that some pathological anchorings can give different behaviors. The free energy surface density of the sample is (in one-constant approximation $K=K_{11}=K_{33}$)

$$F=\int_0^\infty \frac{1}{2}K\left[\left(\frac{d\theta}{dz}\right)^2+\frac{1}{\xi^2}\sin^2\theta\right]dz+\frac{1}{2}\frac{K}{L}\sin^2(\theta_s-\theta_e), \tag{2}$$

where $L=K/A$ is the surface extrapolation length [9] and $\xi=\sqrt{4\pi K/\epsilon_a E^2}$ is the electric field correlation length. The minimization of Eq. (2) gives

$$\left(\frac{d\theta}{dz}\right)^2=C_1+\frac{1}{\xi^2}\sin^2\theta \tag{3}$$

and $C_1=0$ from $\theta(z\to\infty)=0$. Substituting Eq. (3) in Eq. (2) we obtain the torque equilibrium equation

$$\frac{1}{L}\sin[2(\theta_e-\theta_s)]=\frac{2}{\xi}\sin\theta_s. \tag{4}$$

The graphic solutions of this equation are presented in Fig. 2(a) (for $\Psi=0$) and Fig. 2(b) (for $\Psi\neq 0$). The solutions for θ_s as a function of the applied field are presented, respectively, in Figs. 3(a) and 3(b). The equilibrium value of θ_s is obtained as an intersection of the anchoring torque Γ_s with the bulk torque, presented for four increasing E (decreasing ξ) values. In Fig. 2(a) the solution for θ_s glides over the curve Γ_s, decreasing with increasing field, and for $\xi=L$ (curve 3), becomes exactly zero and does not change any more with further field increases. The anchoring is now broken: $\theta_s=0$ corresponds to a *maximum* of the anchoring energy, i.e., $\mathbf{n}_s$ is along the difficult axis $\mathbf{d}$, and the surface

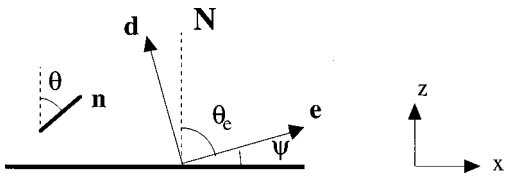

FIG. 1. Geometry of the anchoring.

*Permanent address: Institute of Solid State Physics, Bulgarian Academy of Sciences, Sofia 1784, Bulgaria.

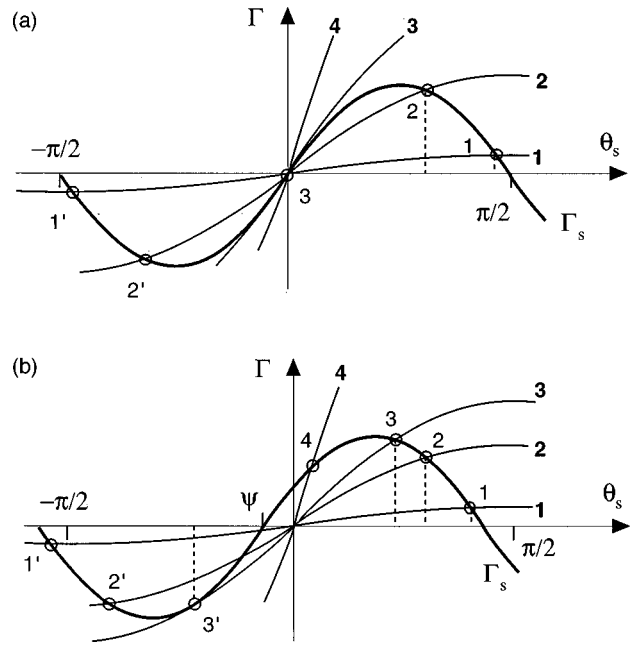

FIG. 2. Graphic solution of Eq. (4). Γ_s is the surface anchoring torque and the curves 1–4 show the integrated bulk torque at increasing fields. (a) Planar anchoring ($\Psi=0$). Curve 3 corresponds to $\xi=L$, the threshold for the anchoring breaking. (b) Tilted anchoring. There is no breaking threshold in this case.

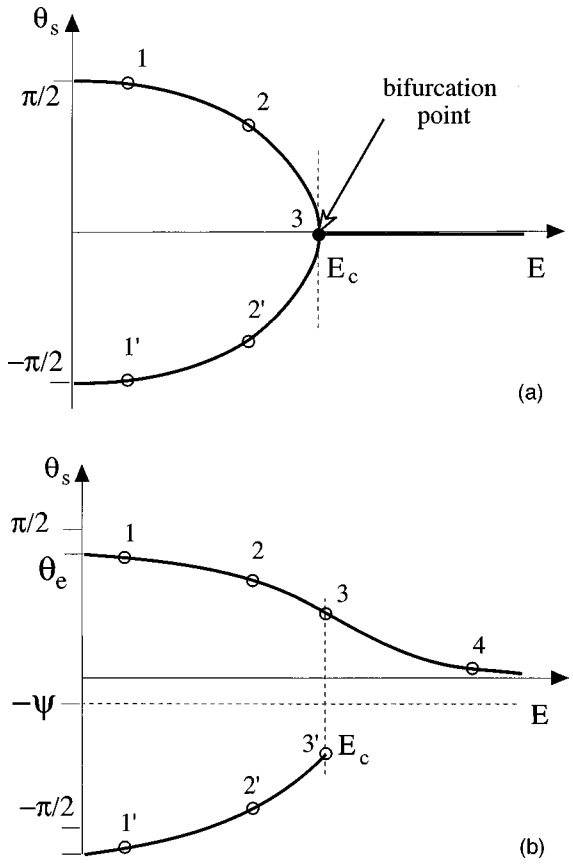

FIG. 3. Surface orientation under field. (a) Planar anchoring. At $E=E_c$ there is second-order anchoring breaking. The two symmetric branches at $E<E_c$ join together at the bifurcation point at $E=E_c$, defined by $\xi=L$. (b) Tilted anchoring. The two branches are asymmetric and correspond to different θ_s and different energies. There is no bifurcation and no anchoring breaking while the solution is on the positive branch. An irreversible first-order transition is possible starting from the negative branch.

torque is *exactly* zero. We note that for the planar anchoring case, by symmetry, there is twofold degeneration of the solutions: θ_s and $-\theta_s$ are both solutions of Eq. (4) and they correspond to the same total energy of the system. The anchoring breaking in this case can be described as a *second-order* phase transition, with order parameter $\sin\theta_s$ [Fig. 3(a)]. At $E\geqslant E_c$, $\sin\theta_s=0$ and the phase is ''disordered.'' When $E<E_c$, two symmetric solutions exist, realized at random. In decreasing field $E=E_c$ is a bifurcation point: the system chooses at this point which solution to realize and it is extremely sensitive to external perturbations. As demonstrated recently [5], the anchoring breaking and the surface bifurcation of planar anchorings can be used to achieve fast bistable bulk texture transitions, controlled by weak couplings.

In the case of tilted anchorings the surface behavior under field changes drastically, due to the lower symmetry [Fig. 2(b)]. Even for very strong fields (curve 4), θ_s is different from zero, the surface torque remains finite, and there is no transition: the anchoring does not break. Negative solutions also exist in this case [Figs. 2(b) and 3(b)], but the two branches are not symmetric [Fig. 3(b)], the positive one corresponding to lower energy. Moreover, if the torque is due only to an electric field applied along **N**, the negative branch is never explored: the molecules rotate to the left in Fig. 2(b) and θ_s decreases as on the positive branch in Fig. 3(b). This is why it is generally believed that the tilted anchoring *cannot be broken*.

Now we will discuss the evolution of the system when it explores the negative branch in Fig. 3(b). Suppose that by some additional field we rotate the molecules slightly to *the right*, starting from $\theta_s=\theta_e-\pi$, as shown in Fig. 4. Once $\theta_s>-\pi/2$ is achieved [e.g., the state $2'$ in Figs. 2(b), 3(b), and 4], the dielectric torque changes its sign and now the electric field alone is sufficient to assure the evolution of the system along the negative branch. We can then neglect for the time being the additional field. At increasing **E** the molecules rotate further toward **N**, approaching the difficult axis, which is in this case *on the way* of the director to the normal. When $\mathbf{n}_s$ becomes too close to **d**, the anchoring torque Γ_s is too weak to equilibrate the strong bulk torque [$3'$ in Figs. 2(b), 3(b), and 4]: the system rapidly crosses the ''forbidden'' zone $3'3$, where torque equilibrium is impossible, and reaches a new equilibrium at point 3 on the positive branch. On further variation of **E** the surface director remains trapped between **N** and **e** and never returns back to the left of

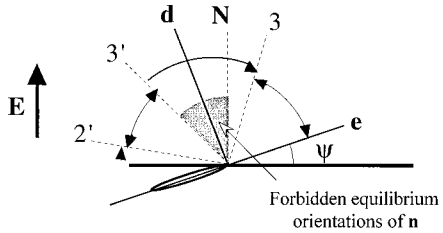

FIG. 4. First-order anchoring breaking. At the beginning an additional external torque is needed in order to obtain the orientation $2'$. For the rest of the process the electric torque alone is sufficient.

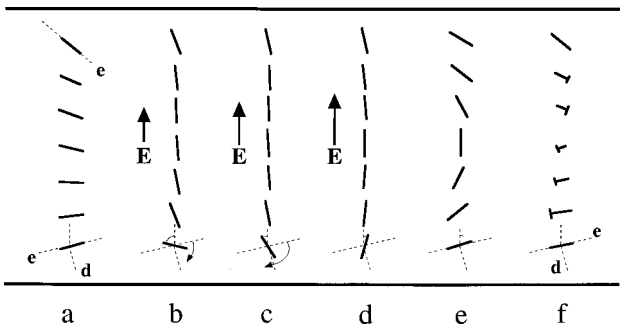

FIG. 5. Anchoring breaking in an inverse pretilt cell. Due to the initial splay texture (a), under increasing field the planar region close to the lower plate is expelled from the cell (b)–(d). The breaking takes place between (c) and (d). After shutting off the field, an additional π deformation is blocked in the sample: bend (e) or twist (f).

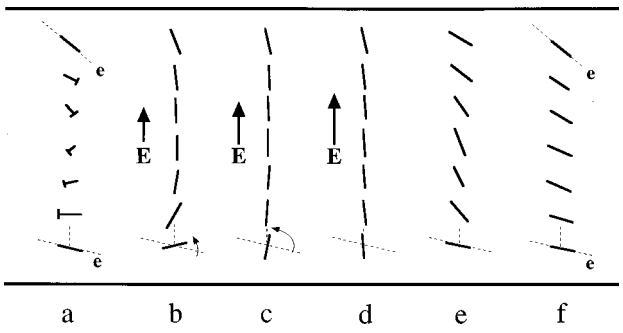

FIG. 6. Anchoring breaking of π-twisted cell with parallel pretilts.

the normal. When the field is finally shut off, the molecules on the surface have performed a half turn (from $\theta_e-\pi$ to θ_e). In a real cell contained between two substrates, this will result in a texture change.

The above scenario describes an anchoring breaking. The electric field induced transition from the negative to positive branch in Figs. 2(b) and 3(b) can be understood as a discontinuous (first-order) phase transition. The system jumps rapidly across the difficult axis, where the bifurcation is expected to be, but does not stop there, being out of equilibrium. Unlike the planar anchoring case, in this first-order breaking the surface never has a choice of the path: the transition from $\theta_s<0$ to $\theta_s>0$ is *forced* by the field. Moreover, this transition is irreversible by the electric field alone. We need again additional torque to start the transition once more.

Several different effects can be used in order to provide the torque inversion for the breaking transition initialization: magnetic field, gradient electric field, elastic coupling with the anchoring on the edges of the pixel, hydrodynamic flow alignment, and so on. These effects can be useful for the study of the anchoring transition, but their application in real devices is limited by their irreproducibility and/or technological problems. Here we propose a very simple and reliable way to provide the inverse torque: the elastic coupling of appropriately chosen tilted anchorings on the two plates. Let us consider the splay texture [Fig. 5(a)] obtained at $E=0$ in a sample with inverse pretilt on the plates. We suppose here that both the pretilt and the anchoring strength are higher on the upper plate than on the lower one. It is well known [10–12] that under weak electric field the texture is transformed as in Fig. 5(b), with the planar ($\theta_s\sim-\pi/2$) region compressed close to the lower tilt plate. In this strongly distorted region, with **n** perpendicular to the field, is stocked a large electric and elastic energy $\sim\pi K/\xi$. With increasing field this energy becomes comparable to the anchoring energy. To minimize the energy, the bulk tries to *expel* the planar region through the plate, making it *virtual*. The bulk torque transmitted to the surface now has the sign needed for the first-order anchoring breaking: the molecules rotate to the right. With increasing **E** the bulk torque becomes stronger [Fig. 2(c)] and the molecules approach the difficult axis **d**. At $E=E_c$, the first-order anchoring breaking threshold, the director rapidly crosses **d** and **N** before finding a new equilibrium [Fig. 5(d)]. If **E** is now shut off, the sample relaxes to the half-turn bend texture [Fig. 5(e)] and then to the π-twisted texture [Fig. 5(f)] having lower energy, due to the usual elastic anisotropy of the nematics. In principle, the calculation of the critical field is more complicated for two coupled plates than for one isolated surface: the solutions of the Euler-Lagrange equation in this case are elliptic functions and not simple exponentials. However, to break the anchoring one needs a strong field, defined by $\xi\approx L\ll d$, the cell thickness. Then the elastic coupling of the plates, proportional to exp $(-d/\xi)$, becomes negligibly small and the torque equilibrium on the lower plate is again described by Eq. (4). At the transition, the two curves in Fig. 2(b) are tangential at point $3'$, giving

$$-\frac{1}{L}\cos 2(\theta_e-\theta_s)=\frac{1}{\xi_c}\cos\theta_s. \tag{5}$$

From Eqs. (4) and (5) we can find the critical values ξ_c and θ_c at which the transition takes place. For example, for $\Psi=\pi/2-\theta_e\ll 1$ we obtain

$$\theta_c\cong-\sqrt[3]{\Psi},\quad \xi_c^2\cong L^2(1+3\Psi^{2/3}), \tag{6}$$

i.e., the critical angle at which the transition occurs [point $3'$ in Fig. 2(b)] is much higher than the pretilt Ψ, but the critical field is approximately the same as in the planar case, defined by $\xi_c\sim L$.

The anchoring breaking in Fig. 5 is activated by the planar region contained in the initial texture. The final texture after the transition [Fig. 5(e) or 5(f)] has no planar zone and the process is irreversible: one cannot go back to the initial splay texture by new anchoring breaking (however, the texture will spontaneously go back slowly, by defect nucleation and propagation). Also, if one starts with a uniform nematic texture, defined by parallel pretilts on the plates, anchoring breaking is impossible: there is no planar zone and under electric field the director rotates everywhere in the sample toward the normal **N** and never toward the plate. If with the same pretilts one starts from a π-twisted texture [Fig. 6(a)], e.g., using appropriated long pitch cholesteric, anchoring breaking is again possible, due to the planar region blocked in the cell. The transition is the same as before (Fig. 5), apart from an additional π twist (Fig. 6). Once more the transition is one way: one cannot go back by anchoring breaking.

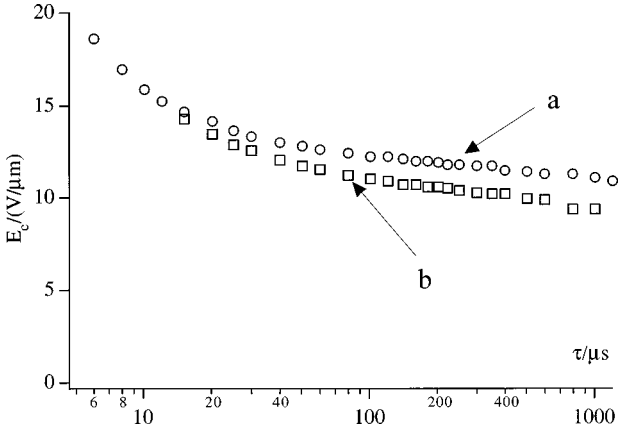

FIG. 7. Anchoring breaking threshold field as a function of the pulse duration τ. (a) Pure 5CB in the geometry of Fig. 5. (b) Chiralized 5CB in the geometry of Fig. 6.

To check our model we prepared thin cells, between two identical plates, covered with evaporated SiO layer (thickness 10 nm, grazing incidence 85°). The tilt on the plates was $20\pm1°$, measured by the method of Lelidis *et al.* [13]. The cells were not glued, in order to enable the rotation of one of the plates relative to the other and to change the sample thickness between 1 and 8 μm, remaining physically with the same anchoring and in the same surface region. The thickness of the cells was measured comparing the birefringence of the sample with the one in a cell with calibrated thickness and the same anchorings. The electric field was applied normal to the plates using transparent ITO electrodes. Square pulses with duration τ and amplitude $\pm U$, or alternative field with a square envelope and effective amplitude U, gave the same results: in our symmetric cells the polar effects are negligible. We then present here all these cases as one and the same.

The first series of samples was prepared using the pure commercial nematic 5CB. In the cells with inverse pretilt, such as in Fig. 5(a), we observe fast textural transitions above some critical voltage $U_c(\tau)$, depending on the pulse duration and the sample thickness. For $U<U_c$ no permanent texture change is observed after the pulse. For $U>U_c$, after the pulse we observe over all the surface of the sample a new texture, identified by its optical behavior as being the half-turn twisted texture of Fig. 5(f).

Several observations confirm that the transition is realized by anchoring breaking. Topologically, the textures [Figs. 5(a) and 5(f)] are incompatible and the transition between them cannot be done by continuous bulk deformation. We can also reject the hypothesis that the transition under field is due to defect propagation: there is no local change of texture around the regions where defects are easily created. Also, the transition takes place over all the sample surface even for a pulse duration of 5 μs, extremely short compared to the characteristic time of the defect-mediated transition observed in low fields (between 10 s and 10 ms depending on the field).

Varying the sample thickness d we found that the observed critical voltage is proportional to d, i.e., that we have thickness independent *field threshold* $E_c(\tau)$, as expected from our model. One typical $E_c(\tau)$ curve is presented in Fig. 7, measured at room temperature for a $d=1{,}96$ μm cell. This curve is qualitatively similar to the dynamical breaking threshold measured for planar anchorings [5]. However, the τ dependence of the threshold is slightly different for the first-order anchoring breaking, due to the different dynamics of the surface. This dynamics is now under study, both theoretically and experimentally, and will be presented separately. At long τ the critical field almost saturates to the static threshold $E_c(\infty)$, in our case about 11 V/μm. For 5CB this corresponds to $\xi_c\cong20$ nm, defining the order of magnitude for the surface extrapolation length $L\cong\xi_c$. This value is similar to the one measured for planar SiO alignments, by anchoring breaking [5] or by the strong field technique [14].

After the measurement of the breaking threshold one of the plates was rotated at angle π in order to obtain a cell with parallel pretilts and uniform tilted texture, without a planar zone. We never observed texture transitions in this kind of cell, even with fields 2 to 3 times higher than $E_c(\tau)$. This also confirms our model and shows that the first-order transition is initialized only when the starting texture contains a region with **n** parallel to the plates in the bulk.

Other cells were prepared with cholesterized nematic (5CB with a chiral dopant). The pitch of the mixture was chosen to minimize the energy of the half-turn twisted texture, such as the textures in Figs. 5(f) and 6(a). Once more, our predictions were confirmed. When the texture contained the planar zone [Fig. 6(a)] we observed anchoring breaking (curve 2 in Fig. 7). For the uniformly tilted texture of Fig. 5(f) we never observed any transition up to fields much higher than E_c. We note that the slightly different curve $E_c(\tau)$ in this case is mainly due to the few percent of dopant in 5CB, which changes slightly the material properties.

In our model we have supposed that during the breaking the director remains in the zenithal plane. However, if the azimuthal anchoring is weak, an azimuthal breaking transition is possible under the weak back flow torque. To reject this hypothesis, we note that the hydrodynamic coupling always favors the final π-twisted state [5], independent of the initial texture, in strong disagreement with our observations. The negligible effect of the back flow for the breaking of the tilted anchoring is due mainly to the fact that the surface torque never vanishes and dominates the hydrodynamic one which is much weaker. Also, in our particular case the azimuthal anchoring is very strong, with an extrapolation length shorter than 50 nm, estimated by the technique of Ref. [15].

Our assumption of no azimuthal distortions can also fail if a coupling between the azimuthal and the zenithal anchorings exists. For example, for SiO coatings close to the bistable transition [16], one can obtain an azimuthal deviation applying a zenithal torque. By symmetry we do not expect this kind of behavior for our monostable tilted anchorings when the director deviation from the easy axis is small. However, we cannot exclude it at the breaking transition, when **n** is almost along the difficult axis **d**. Depending on the details of the anchoring energy function around **d**, unknown for the time being, **n** can stay in the xz plane, or can go around **d**, introducing some twist close to the substrates. Even in this case the behavior of the breaking transition will not change qualitatively: by symmetry it should remain a first-order transition, initialized by the inverse pretilts and irreversible by the same effect. We expect that the dynamical experiments under progress will enable the detailed study of the anchoring at strong torques.

In conclusion, we proposed a mechanism for breaking of tilted nematic anchorings using an electric field normal to the plates. This kind of surface anchoring breaking is shown to be a discontinuous first-order transition. We show that the elastic coupling of the tilted orientations on both plates can be used to provoke the first-order transition. We observe the breaking experimentally by fast (in the μs range) bulk texture changes, resulting in additional π twist in the final state. The rapidity of the breaking transition can be useful for display applications. We continue our studies on the dynamics of the breaking and on the possibilities to control the choice of the final state by additional couplings, e.g., the hydrodynamical coupling already used in the case of planar anchorings [5].

We are grateful to G. Durand for fruitful discussions.

[1] N. A. Clark and S. T. Lagerwall, Appl. Phys. Lett. **36**, 899 (1980).
[2] R. Barberi and G. Durand, Appl. Phys. Lett. **58**, 2907 (1991).
[3] R. Barberi, M. Giocondo, and G. Durand, Appl. Phys. Lett. **60**, 1085 (1992).
[4] R. Barberi, M. Giocondo, Ph. Martinot-Lagarde, and G. Durand, Appl. Phys. Lett. **62**, 3270 (1993).
[5] I. Dozov, M. Nobili, and G. Durand, Appl. Phys. Lett. **70**, 1179 (1997).
[6] G. Barbero and R. Barberi, J. Phys. (Paris) **47**, 609 (1983).
[7] G. Barbero, N. V. Madhusudana, J. F. Palierne, and G. Durand, Phys. Lett. **103A**, 385 (1984).
[8] A. Rapini and M. Papoular, J. Phys. (Paris), Colloq. **30**, C4-54 (1969).
[9] P. G. de Gennes, *The Physics of Liquid Crystals* (Clarendon, Oxford, 1974).
[10] J. Cheng, R. N. Thurston, and D. W. Berreman, J. Appl. Phys. **52**, 2756 (1981).
[11] J. Cheng, R. N. Thurston, G. D. Boyd, and R. B. Meyer, Appl. Phys. Lett. **40**, 1007 (1982).
[12] R. N. Thurston, J. Cheng, and G. D. Boyd, J. Appl. Phys. **53**, 4463 (1982).
[13] I. Lelidis, A. Gharbi, and G. Durand, Mol. Cryst. Liq. Cryst. **223**, 263 (1992).
[14] H. Yokoyama, S. Kobayashi, and H. Kamei, J. Appl. Phys. **61**, 4501 (1987).
[15] E. Polossat and I. Dozov, Mol. Cryst. Liq. Cryst. **282**, 223 (1996).
[16] M. Nobili and G. Durand, Europhys. Lett. **25**, 527 (1994).